Journal of Materials Chemistry C

Accepted Manuscript

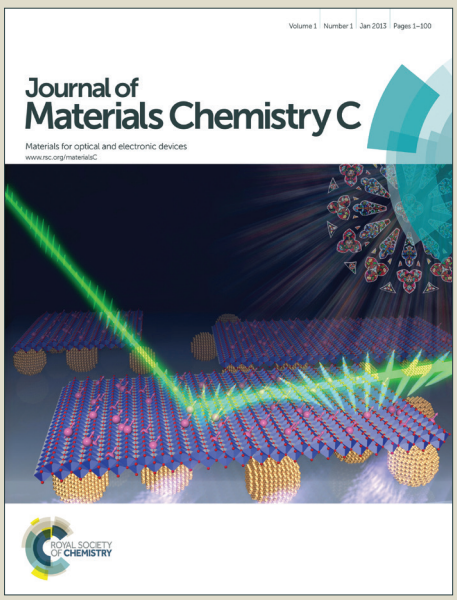

ROYAL SOCIETY OF CHEMISTRY

www.rsc.org/materialsC

Journal of Materials Chemistry C

COMMUNICATION

Room Temperature Fabrication and Patterning of Highly Conductive Silver Features using In-Situ Reactive Inks by Microreactor-Assisted Printing

Received 00th January 20xx,
Accepted 00th January 20xx

DOI: 10.1039/x0xx00000x

www.rsc.org/

Chang-Ho Choi,[a] Elizabeth Allan-Cole,[a] and Chih-hung Chang[a]

Highly conductive silver was fabricated at room temperature using in-situ reactive silver precursor inks by microreactor-assisted printing without any post-processing. Reactive silver nanoinks, synthesized *in-situ* from the microreactor, were directly delivered onto glass and polymeric substrates without any surface treatment to form a highly dense and uniform silver feature. The distribution of the reactive silver nanoinks can be controlled simply by adjusting the flow rate of the continuous flow system. Silver lines were fabricated using the *in-situ* reactive precursors delivered via a micro-channel applicator. The electrical conductivity of the silver film and feature were measured to be around 3.3 × 10^7 (S/m), corresponding to about half of the conductivity of bulk silver. The functionality of the silver line was confirmed through the operation of LEDs. This study demonstrates the possibility to fabricate patterned silver features at room temperature from *in-situ* nanoinks without the aid of any post-processing.

Silver possesses excellent electrical conductivity, surface plasmon resonance (SPR), and high reflectivity, leading to a variety of applications in microelectronic circuitry, gas sensors, low emissivity coatings, and more recently as transparent conductive electrodes for displays.[1-6] Since the properties of silver features are closely associated with synthetic approaches, many different synthetic methods have been developed to yield high quality silver features. Direct printing in an atmospheric environment offers a potentially low-cost and materials-efficient method for manufacturing silver features for electronics and energy devices. Significant efforts and progress have been made in developing printable silver inks. Nanoparticle suspensions and organo-metallic compounds are the two primary precursors. Many research groups have reported highly conductive silver features using silver nanoparticle inks after annealing at approximately 200-350 °C. Lewis and co-workers reported omnidirectional printing of remarkable silver features using colloidal silver nanocrystal inks where organic stabilizers were needed to create a stable silver nanoparticle suspension.[7] A post-sintering process is required after the printing to remove organic stabilizers that usually decompose at temperatures higher than 200 °C.[8, 9] Enormous efforts have been made to further reduce the sintering temperature by developing novel silver precursor inks. Kao et al. reported a clever use of two ink channels to implement the silver mirror reaction.[9] The electrical conductivity of the resulting silver lines was 6% of bulk silver at room temperature. Perelaer *et al.* used microwave flash sintering to shorten the sintering duration of printed silver nanocrystals and achieved highly conductive silver films after microwave sintering for 150 seconds.[10] Reinhold *et al.* showed the use of argon plasma sintering to fabricate the silver film on a plastic substrate at a substrate temperature of 120 °C. [11] Layani *et al.* developed self-sintering silver nanoparticles after a short exposure to HCl vapors to achieve the high electrical conductivity path at room temperature.[12] Olkkonen *et al*. established the sintering of inkjet printed silver tracks with boiling salt water.[13] Dearden *et al.* showed that silver with good conductivity could be obtained at a relatively low temperature of 150°C using organo-silver ink.[14] Most recently, Walker *et al.* developed reactive particle-free silver inks by modifying the Tollens' reagent.[15] Silver features with high conductivity were obtained after 100 °C heat treatment. These innovative approaches are capable of producing highly conductive silver features at relatively low temperatures. However, there are still areas for improvement. The synthesis of well- dispersed silver nanoparticle and organic metallic inks suitable for printing and low temperature sintering with sufficient stability usually requires the stringent selection of reactants for successful synthesis, sufficient stability to ensure ink shelf-life, and tedious synthesis procedures that would increase cost. [16, 17] In addition, the sintering processes require additional power sources and facilities.

[a] *Oregon Process Innovation Center/ Microproduct Breakthrough Institute and School of Chemical, Biological & Environmental Engineering, Oregon State University, Corvallis, OR 97331, United States*

†Electronic Supplementary Information (ESI) available: Experimental procedures to produce the silver film and silver line, Speciation diagram of silver precursors, Table to exhibit comparison of electrical conductivity of reported silver film with one discussed in this study.

In this communication, we report, for the first time, the fabrication of highly conductive silver features at room temperature using *in-situ* reactive precursor inks generated by a novel microreactor-assisted printing technique without any post processing steps. The invention of this methodology aims at achieving one of more efficient and economical way in manufacturing highly electrical conductive silver featurs. Compared to other printing techniques that gnerally necessiate organic stablizers, our process allows for printed silver features using *in-situ* reactive silver precursor inks without using organic stablizers. In addition, since silver precursor inks are free of organic stabilizers, neither post-annealing process nor other post-surface treatment are required to achieve an excellent conductive path. A Tollens' process offers some advantages in preparing silver films, including simplicity, low cost, and low temperature requirements.[18, 19] Particularly the Tollens' process allows for the silver film formation in the absence of organic stabilizers. However, the typical Tollens' reaction is based on the batch process, resulting in some inherent problems such as homogeneous particle formation and difficulty in reaction selectivity that consequently results in non-uniform film formation. We have used a microreactor-assisted process to control a modified Tollen's reaction to generate *in-situ* silver precursor inks to resolve some of these issues. In a continuous flow microreactor, reaction kinetics can be controlled by simply adjusting process parameters. For example, by properly tuning the flow rate of solution, which in turn controls the residence time, we were able to obtain various reactive precursors such as reactive molecular species, individual nanocrystals, or nanocrystals assemblies.[20, 21] These reactive precursors were then delivered immediately onto a surface to enable surface reaction and/or assembly.[22, 23] The modified Tollens' reagent was prepared by dissolving silver nitrate ($AgNO_3$) into deionized water containing ammonium hydroxide (NH_4OH). A speciation diagram was constructed to find the pH range where high purity Tollens' reagent ($Ag(NH_3)_2^+$) is generated (Fig. S1). The pH range from 9 to 12 was found to be appropriate for the $Ag(NH_3)_2^+$ formation according to the speciation diagram, and the experimental pH value was measured to be right around 11. Formaldehyde (HCHO) was used as a reductant. The detailed experimental procedures are described in the supporting information. Reactive silver precursor inks were generated *in-situ* as the Tollens' reagent, the $Ag(NH_3)_2^+$ solution, was mixed with the formaldehyde solution via a micromixer. The silver mirror reaction takes place following: $HCHO+2[Ag(NH_3)^2]^++2OH^-\rightarrow HCOONH_4+2Ag+3NH_3+H_2O$.[24]

We carried out the analysis using UV-Vis absorption measurements to investigate the kinetics of silver precursor ink formation in real time. The UV-Vis absorption spectra at different mean residence times, controlled by the flow rate, are given in Fig. 1. The flow rate of 0.4 mL min^{-1}, 0.65 mL min^{-1}, and 0.73 mL min^{-1} correspond to a residence time of 118 seconds, 74 seconds, and 65 seconds respectively. It can be seen clearly from the spectra that an absorption peak between 400 and 450 nm is growing at longer residence time. This absorption is associated with the surface plasmon of silver nanocrystals. This result is consistent with the silver mirror reaction starting from the generation of silver atoms, followed by the formation of small nuclei and subsequently silver nanocrystals. Based on the result of real time absorption spectrum in Fig. 1, a flow rate of 0.4 mL min^{-1} was adopted to fabricate silver films and features. At a flow rate of 0.4 mL min^{-1}, the absorption peak with a high intensity was observed, indicating increased concentration of silver nanocrystals. It was found that the conductive silver features cannot be formed at higher flow rates (e.g. 1.5 mL min^{-1}). At such a high flow rate, the residence time is not long enough to form primary silver nanocrystals, building blocks for the film formation. Instead silver atoms or clusters are considered to be major products at this flow rate, which only yielded a discontinuous film (Fig. S2). And at a flow rate below 0.4 mL min^{-1} (e.g. 0.1 mL min^{-1}), silver nanocrystals would experience the aggregation, causing the non-uniform film formation. In order to acquire the silver film with highly electrical conductivity, the film uniformy is an important factor. These results demonstrate that finding an optimal flow rate (i.e. residence time) is very important in achieving uniform and conductive silver films and features. It is believed that at a flow rate of 0.4 mL min^{-1}, the colloidal silver nanocrystals along with atomic silver and silver clusters were synthesized for the silver feature deposition.

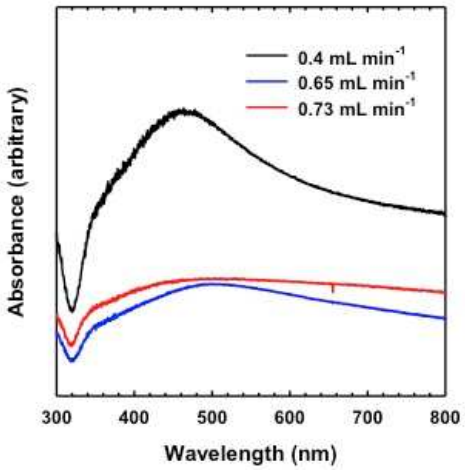

Fig. 1. Real time analysis of optical properties of silver inks at various flow rates.

Fig. 2 shows the TEM characterizations of silver nanocrystals, building blocks for the silver feature formation, synthesized at room temperature. The TEM image shows well-dispersed, spherical silver nanocrystals with a size mostly ranged from 2 to 10 nm in diameter. A nanocrystal size distribution is also analyzed in Fig. 2d. The SAED pattern indicates the high crystallinity of silver nanocrystals, showing clearly distinct ring patterns. The dominant diffraction patterns are indexed, which agrees well with typical silver nanocrystals. A typical silver nanocrystal with approximately 10 nm in

diameter was examined at high magnification. Lattice fringes are clearly observed, confirming the high crystallinity of silver nanocrystals.

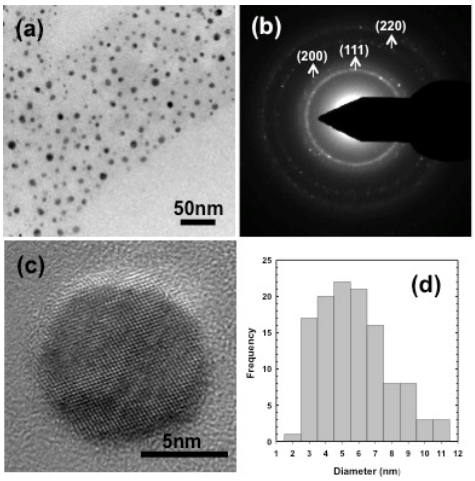

Fig. 2. Characterizations of silver nanocrystals: (a) TEM image of silver nanocrsytals, (b) SAED pattern of silver nanocrystals, (c) a typical silver nanocrystal, and (d) nanocrystal size distribution.

Fig. 3 displays the characterization results of the silver film obtained after a 15 minute deposition using silver nanoinks generated *in-situ* from the microreactor at a flow rate of 0.4 mL min^{-1}. The deposition procedures are described in the supporting information (Fig. S3). The silver film is composed of a number of spherical nanocrystals (Fig. 3a). The grain size of the nanocrystal varies from several tens of nanometers to several hundreds of nanometers in diameter. These nanocrystals connected with one another in a densely packed film without forming any voids, providing excellent electrically conductive paths. The cross sectional SEM image of the silver film is shown in Fig. 3b. The thickness of the silver film is uniform, and the average thickness was measured to be around 134 ± 9 nm. It is believed that primary silver nanocrystals served as building blocks for the framework formation of the film by closely connecting one another while silver clusters along with silver atoms filled the voids between the primary silver nanocrystals, which eventually produced the dense single layer film. We were able to estimate the concentratration range of primary silver nanocrystals synthesized in microreactor by correlating the volume of the silver solution dispersed for the film formation with the volume of the formed film. Assume that the total silver solutions were only consumed to form the film. The silver solution volume of 6 mL was consumed to fabricate the silver film with total volume of 5.4×10^{-13} m^3. With an assumption of perfect sphere of primary silver nanocrystals, the concentration range of the nanocrystals can be estimated to be around betweem 2.73×10^{12} /mL and 2.15×10^{10} /mL. The upper limit and lower limit of the estimated concentratios corresponds to the size of the nanocrystals with 2 nm and 10 nm respectively. The highly dense silver nanocrystalline film was further confirmed by the AFM analysis shown in Fig. 3c. The average roughness was measured to be around 13.9 nm. The XRD pattern of the silver film indicates the high crystallinity of the film, exhibiting sharp peaks with high intensity. The diffraction peaks are attributed to the face-centered cubic (fcc) crystalline structure of Ag (JCPDS No.89-3722). The XRD pattern is in accordance with the SAED pattern observed in Fig. 2b. We also successfully demonstrated the deposition of silver films on polymeric substrates at room temperature. Fig. 3e shows an optical image of a highly reflective silver film on a flexible polyimide substrate.

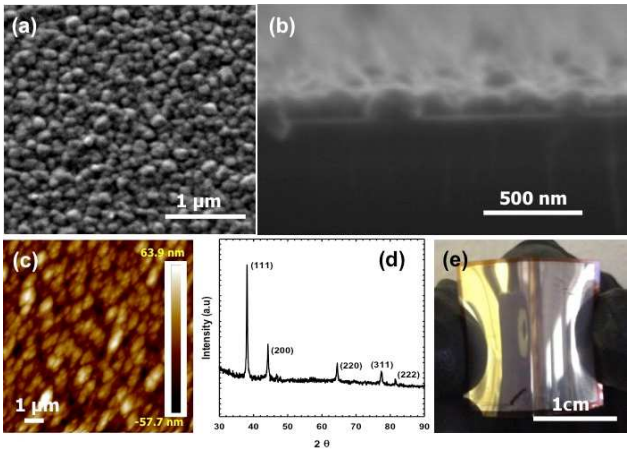

Fig. 3. Characterizations of the silver film: (a), (b) Plain view and cross sectional area SEM images, (c) AFM image, (d) XRD pattern of the as-deposited silver film.,(e) Optical image of the silver film deposited on a flexible polyimide substrate.

To fabricate patterned silver features via the microreactor-assisted printing, we used a microchannel applicator. The microchannel, a critical part of the microchannel applicator, was fabricated *via* a hot embossing technique. The micro hot embossing technique, known to be an effective replication approach to fabricate micro- and nanoscale features with high accuracy, has been widely used for various applications in industry.[25, 26] We fabricated a microchannel applicator featured with a microscale single line. We also prepared a flow cell that is assembled with the microchannel to provide an inlet and outlet for silver inks during the silver deposition. Detail on the silver line deposition using the microchannel applicator is described in the supporting information (Fig. S4). Through the microchannel applicator, silver inks synthesized in the microreactor were guided to flow over the substrate to form a silver line feature. (Fig. 4). This method can be used to create smaller, more complex features with more advanced application methodologies.

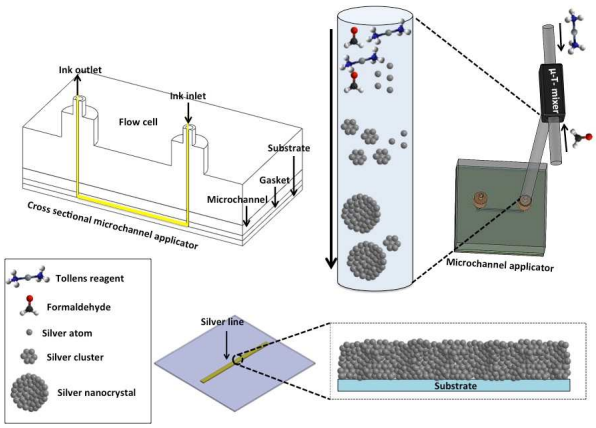

Fig. 4. Schematic diagram of manufacturing silver line.

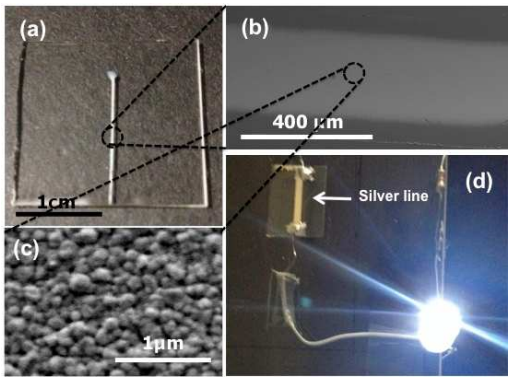

Fig. 5. Characterizations of silver line: (a) optical image of the silver line on glass substrate, (b) and (c) low and high-resolution SEM images of silver line, and (d) optical image of LED.

Fig. 5a~c exhibits the results of the silver line deposition on a glass substrate. The silver line is 2 cm in length and approximately 300 μm in width. The SEM image of the silver feature shows a well-defined silver line that consists of continuous, densely packed silver nanograins. The electrical conductivity of the both the as-deposited silver film and line feature were measured to be 3.3×10^7 S/m at room temperature. The conductivity is around half of the value of bulk silver. The electrical conductivity of our silver feature shows one of the highest values among silver features prepared at room temperature. Table S1 in the supporting information lists a number of state-of-the-art results of printed silver features. It is worth noting that our silver feature was fabricated at room temperature without any post-sintering steps. Kao *et al.* reported an impressive result of a printed silver feature with a 6% conductivity of bulk silver at room temperature using reactive two channel ink jet system.[7] Layani and Magdassi reported a clever approach to fabricate silver grids by guided self-assembly of silver nanoparticles following by chemical sintering using HCL at room temperature. An impressive conductivity value of $1x10^7$ S/m was obtained.[10] The electrical conductivity of the silver feature fabricated by the microreactor-assisted printing was demonstrated using LEDs (Fig. 5d).

In conclusion, uniform and highly conductive silver films and features were fabricated at room temperature using reactive silver nanoinks generated from a continuous flow microreactor. Reactive silver solution generated *in-situ* from the microreactor were directly delivered onto the substrates to form the silver films. Builidng blocks for the film formation, including dispersed silver nanocrystals and silver clusters, were selectively obtained by using a flow rate of 0.4 mL min^{-1}. The silver nanocrystals formed the framework of the film and the silver clusters filled the voids formed between silver nanocrystals, which resulted in continuous and unifrom films. Patterned silver features were fabricated using a novel microreactor-assisted printing technique by delivering the reactive silver nanoinks to a surface via a flexible microchannel applicator. A 300 μm wide silver line was demonstrated. The resulting silver film and line show electrical conductivity values about half of the bulk silver value. This study demonstrates the capability of a novel microreactor-assisted printing technique to fabricate highly conductive silver features at room temperature without the aid of a post-sintering process for the first time. This was achieved by using *in-situ* reactive silver nanoinks generated from stable, long-shelf life, low-cost, commercially available precursors.

Acknowledgement

We like to acknowledge the assistance of Yujuan He and Changqing Pan (OSU) in fabricating the micro embosser; Andy Brickman (OSU) to build the circuit for LEDs; and Peter Kreider for valuable comments. We like to thank the financial supports from Oregon BEST commercialization grant, NSF I-Corps IIP-1439485, NSF MRI-1040588. Elizabeth Allan-Cole is grateful for the support of Johnson Scholar Summer Internship.

Notes and references

1 J. Tate, J. A. Rogers, C. D. W. Jones, B. Vyas, D. W. Murphy, W. J. Li, Z. A. Bao, R. E. Slusher, A. Dodabalapur and H. E. Katz, *Langmuir*, 2000, **16**, 6054.
2 D. Kitenge, R. K. Joshi, M. Hirai and A. Kumar, *IEEE Sensors Journal*, 2009, **9**, 1797.
3 M. Moskovits, *Surface-Enhanced Raman Scattering: Physics and Applications*, 2006, **103**, 1.
4 A. Kloppel, W. Kriegseis, B. K. Meyer, A. Scharmann, C. Daube, J. Stollenwerk and J. Trube, *Thin Solid Films*, 2000, **365**, 139.
5 C. Gao, Y. Hu, M. Wang, M. Chi and Y. Yin, *J. Am. Chem. Soc.*, 2014, **136**, 7474.
6 C. Gao, Z. Lu, Y. Liu, Q. Zhang, M. Chi, Q. Cheng and Y. Yin, *Angew. Chem. Int. Ed.*, 2012, **51**, 5629.
7 B. Y. Ahn, E. B. Duoss, M. J. Motala, X. Guo, S.-I. Park, Y., Xiong, J. Yoon, R. G. Nuzzo, J. A. Rogers and J. A. Lewis, *Science*, 2009, **323**, 1590.
8 H. C. Kim, T. L. Alford and D. R. Allee, *Appl. Phys. Lett.*, 2002, **81**, 4287.
9 Z.-K. Kao, Y.-H. Hung and Y.-C. Liao, *J. Mater. Chem.*, 2011, **21**, 18799.
10 J. Perelaer, M. Klokkenburg, C. E. Hendriks and U. S. Schubert, *Adv. Mater.*, 2009, **21**, 4830.
11 I. Reinhold, C. E. Hendriks, R. Eckardt, J. M. Kranenburg, J. Perelaer, R. R. Baumann and U. S. Schubert, *J. Mater. Chem.*, 2009, **19**, 3384.
12 M. Layani and S. Magdassi, *J. Mater. Chem.*, 2011, **21**, 15378.
13 J. Olkkonen, J. Leppaniemi, T. Mattila and K. Eiroma, *J. Mater. Chem. C*, 2014, **2**, 3577.
14 A. L. Dearden, P. J. Smith, D. Y. Shin, N. Reis, B. Derby and P. O'Brien, *Macromol. Rapid. Commun.*, 2005, **26**, 315.
15 S. B. Walker and J. A. Lewis, *J. Am. Chem. Soc.*, 2012, **134**, 1419.
16 S. Kapoor, *Langmuir*, 1998, **14**, 1021.
17 X.-M. Wang, D.-D. Zhou, Q.-Q. Zou and Y.-Y. Xia, *J. Mater. Chem.*, 2012, **22**, 15418.
18 Y. D. Yin, Z. Y. Li, Z. Y. Zhong, B. Gates, Y. N. Xia and S. Venkateswaran, *J. Mater. Chem.*, 2002, **12**, 522.
19 Y. Saito, J. J. Wang, D. A. Smith and D. N. Batchelder, *Langmuir*, 2002, **18**, 2959.
20 C.-H. Choi, Y.-W. Su and C.-h. Chang, *CrystEngComm*, 2013, **15**, 3326.
21 P. H. Mugdur, Y. J. Chang, S. Y. Han, Y. W. Su, A. A. Morrone, S. O. Ryu, T. J. Lee and C. H. Chang, *J. Electrochem. Soc.*, 2007, **154**, D482.
22 C.-H. Choi and C.-h. Chang, *Cryst. Growth.Des.*, 2014, **14**, 4759.
23 S.-Y. Han, B. K. Paul and C.-h. Chang, *J. Mater. Chem.*, 2012, **22**, 22906.
24 K. S. Chou and C. Y. Ren, *Mater. Chem. Phys.*, 2000, **64**, 241.
25 L. Peng, Y. Deng, P. Yi and X. Lai, *J. Micromech. Microeng.*, 2014, **24**, 013001.
26 L. Lin, Y. T. Cheng and C. J. Chiu, *Microsyst. Technol.*, 1998, **4**, 113.
27 E. Zaleta-Alejandre, R. Balderas-Xicotencatl, M.L. Perez Arrieta, A.N. Meza-Rocha, Z. Rivera-Alvarez and C. Falcony, *Mater.Sci.Eng.,B*, 2013, **178**, 1147.
28 J. Perelaer, B.-J. de Gans and U. S. Schubert, *Adv. Mater.*, 2006, **18**, 2101.
29 T. H. J. van Osch, J. Perelaer, A. W. M. de Laat and U. S. Schubert, *Adv. Mater.* 2008, **20**, 343.
30 S. M. Bidoki, D. M. Lewis, M. Clark, A. Vakorov, P. A. Millner and D. McGorman, *J. Micromech. Microeng.*, 2007, **17**, 967.
31 S. B. Fuller, E. J. Wilhelm and J. M. Jacobson, *J. Microelectromech. Syst.* 2002, **11**, 54.
32 J. B. Szczech, C. M. Megaridis, D. R. Gamota and J. Zhang, *IEEE Trans. Electron. Packaging Manufact.*, 2002, **25**, 26.
33 H.-H. Lee, K.-S. Chou and K.-C. Huang, *Nanotechnology*, 2005, **16**, 2436.
34 Z. Liu and Y. Su, K. Varahramyan, *Thin Solid Films*, 2005, **16**, 2436.
35 J. Natsuki and T. Abe, *J. Colloid. Inteface. sci.*, 2011, **359**, 19.
36 S. Jeong, H. C. Song, W. W. Lee, Y. Choi and B.-H. Ryu, *J. Appl. Phys.*, 2010, **108**, 102805.
37 A. Inberg, P. Livshits, Z. Zalevsky, Y. Shacham-Diamand, *Microelectron. Eng.*, 2012, **98**, 570.
38 K.-S. Chou, K.-C. Huang and H.-H. Lee, *Nanotechnology*, 2005, **16**, 779.
39. F. Stellacci, C. A. Bauer, T. Meyer-Friedrichsen, W. Wenseleers, V. Alain, S. M. Kuebler, S. J. K. Pond, S. R. Marder and J. W. Perry, *Adv. Mater.*, 2002, **14**, 194.